Accelerated atherosclerosis caused by serum amyloid A response in lungs of ApoE/ mice

Christophersen, Daniel Vest; Møller, Peter; Thomsen, Morten Bækgaard; Lykkesfeldt, Jens; Loft, Steffen; Wallin, Håkan; Vogel, Ulla; Jacobsen, Nicklas Raun

RESEARCH ARTICLE

Accelerated atherosclerosis caused by serum amyloid A response in lungs of ApoE−/− mice

Daniel Vest Christophersen[1,2,3] | Peter Møller[1] | Morten Bækgaard Thomsen[4] | Jens Lykkesfeldt[5] | Steffen Loft[1] | Håkan Wallin[1,3,6] | Ulla Vogel[3,7] | Nicklas Raun Jacobsen[3] (iD)

[1]Department of Public Health, Section of Environmental Health, Faculty of Health Sciences, University of Copenhagen, Copenhagen K, Denmark

[2]Ambu A/S, Ballerup, Denmark

[3]The National Research Centre for the Working Environment, Copenhagen, Denmark

[4]Department of Biomedical Sciences, Heart and Circulatory Research Section, Faculty of Health Sciences, University of Copenhagen, Copenhagen N, Denmark

[5]Department of Veterinary Disease Biology, Faculty of Health and Medical Sciences, University of Copenhagen, Frederiksberg C, Denmark

[6]National Institute of Occupational Health, Oslo, Norway

[7]Department of Micro- and Nanotechnology, Technical University of Denmark, Kgs. Lyngby, Denmark

Correspondence
Nicklas Raun Jacobsen, The National Research Centre for the Working Environment, Lersø Parkalle 105, Copenhagen 2100, Denmark.
Email: nrj@nrcwe.dk

Abstract

Airway exposure to eg particulate matter is associated with cardiovascular disease including atherosclerosis. Acute phase genes, especially *Serum Amyloid A3* (*Saa3*), are highly expressed in the lung following pulmonary exposure to particles. We aimed to investigate whether the human acute phase protein SAA (a homolog to mouse SAA3) accelerated atherosclerotic plaque progression in *Apolipoprotein E* knockout (*ApoE−/−*) mice. Mice were intratracheally (i.t.) instilled with vehicle (phosphate buffered saline) or 2 µg human SAA once a week for 10 weeks. Plaque progression was assessed in the aorta using noninvasive ultrasound imaging of the aorta arch as well as by en face analysis. Additionally, lipid peroxidation, SAA3, and cholesterol were measured in plasma, inflammation was determined in lung, and mRNA levels of the acute phase genes *Saa1* and *Saa3* were measured in the liver and lung, respectively. Repeated i.t. instillation with SAA caused a significant progression in the atherosclerotic plaques in the aorta (1.5-fold). Concomitantly, SAA caused a statistically significant increase in neutrophils in bronchoalveolar lavage fluid (625-fold), in pulmonary *Saa3* (196-fold), in systemic SAA3 (1.8-fold) and malondialdehyde levels (1.14-fold), indicating acute phase response (APR), inflammation and oxidative stress. Finally, pulmonary exposure to SAA significantly decreased the plasma levels of very low-density lipoproteins - low-density lipoproteins and total cholesterol, possibly due to lipids being sequestered in macrophages or foam cells in the arterial wall. Combined these results indicate the importance of the pulmonary APR and SAA3 for plaque progression.

KEYWORDS

acute phase response, *Apolipoprotein E* knockout (*ApoE−/−*) mice, ischemic heart disease, recombinant human apolipoprotein serum amyloid A (hApo-SAA), Western-type diet

1 | INTRODUCTION

In atherosclerosis, the lumen of arteries narrow due to the buildup of plaques. This may lead to ischemic heart disease, the leading cause of deaths worldwide.[1] Exposure to ambient air particulate matter is associated with increased risk of cardiovascular disease (CVD) in humans.[2] Murine models of atherosclerosis include apolipoprotein E ($ApoE^{-/-}$)[3] and low-density lipoprotein receptor ($Ldlr^{-/-}$) knockout mice.[4] $ApoE^{-/-}$ mice spontaneously develop atherosclerotic lesions with age or when fed a Western-type diet rich in fat, sucrose, and cholesterol.[5] Pulmonary exposure to nanoparticles and fibers has been shown to exacerbate the progression of atherosclerosis in $ApoE^{-/-}$ and $Ldlr^{-/-}$.[6-9] The mechanistic linkage between pulmonary exposure to particles and cardiovascular effects is typically considered to be mediated by oxidative stress and inflammatory signaling from the lung to the circulation.[10] However, recently a causal link between the acute phase response (APR) protein serum amyloid A (SAA) and atherosclerosis was suggested.[11] SAA belongs to the group of APR proteins that are the first line of defense protecting the body from invasion by pathogens (bacterial infections) and trauma by the recruitment of immune cells. APR is defined by increases in, for example, C-reactive protein (CRP), SAA, and fibrinogen and during APR these proteins can increase thousand fold.[12]

The SAA family is evolutionary highly conserved and complexes with high-density lipoproteins (HDL).[13] The *Saa* gene family consists of four isotypes in mice. *Saa1, Saa2, Saa3,* and *Saa4* are expressed in the liver, and *Saa1, Saa2, and Saa3* are also expressed in other distinct tissues including lung (especially *Saa3*)[11,14] and adipose tissue.[15] In humans, *SAA3* is a pseudogene[16] which is a likely reason for the lack of focus in earlier publications. In mice, *SAA3* functions as a neutrophilic attractant and is associated with activation of Toll-like receptor 4.[17] The APR has previously been thought of as mostly of hepatic origin.[18] However, we have shown that pulmonary exposure to nanosized carbon black,[19] titanium dioxide (TiO_2)[20,21] and multi-walled carbon nanotubes (MWCNT)[22,23] increase the APR, with expression of *Serum amyloid A3* (*Saa3*) being the single most upregulated APR gene in the lungs of mice. At the same time, hepatic mRNA expression of *Saa3* is generally low if even present. Concomitantly, it was found that SAA concentrations in plasma were increased after pulmonary exposure to the above mentioned particles.[11,14,19,21,22,24] Such increased concentrations of SAA may mediate particle-induced atherosclerosis, since both short and long-term increases in virus-mediated systemic levels of SAA have promoted plaque formation. This indicates that SAA directly contributes to atherosclerotic progression.[25,26] Recently, it was shown that systemic overexpression of SAA3 in mice accelerated atherosclerosis. Additionally, deficiency of SAA1 and SAA2 had no effect

on atherosclerosis, but additional suppression of SAA3 decreased atherosclerosis.[27] In the lung, *Saa3* expression levels correlate with the inflammation and with the administered particle surface area.[11,21,22] In the blood SAA complexes with HDL, forming SAA-HDL, and thereby alters the structure and function of HDL. Due to deficient reverse cholesterol transport, the SAA-HDL complex promotes foam cell formation from macrophages, whereas the unmodified HDL (Apo-A1-HDL) may actually inhibit foam cell formation by facilitating the cholesterol efflux.[11,28]

We hypothesize that pulmonary expression of SAA3 plays a pivotal role in particle-induced atherosclerosis. Figure 1 depicts the overall hypothesized mechanism of action as well as the steps investigated in the present study. We hypothesized that i.t. instillation of SAA in the lungs of $ApoE^{-/-}$ mice promote neutrophil chemo-attraction and inflammation, leading to a pulmonary driven systemic APR and further downstream to plaque progression (Figure 1). Critical end-points assessed in the present study include inflammation and *Saa3* expression in the lung as well as SAA3, lipid peroxidation and lipid composition in plasma. Plaque progression was investigated in the aortic arch by noninvasive real-time ultrasound imaging in live animals as well as by assessment of the plaque area in the whole aorta using en face analysis.

2 | MATERIALS AND METHODS

2.1 | Chemicals

Vehicle was sterile Dulbecco's phosphate-buffered saline (PBS) (cat.no. 02-023-1A Biological Industries, Israel). Recombinant human Apo-SAA protein was purchased from PeproTech Inc (PeproTech, Inc, USA). Human Apo-SAA has a high purity (≥98%) and very low endotoxin content (<1 EU/μg). The amino acid sequence of the recombinant hApo-SAA was the following: MRSFFSFLGE AFDGARDMWR AYSDMREANY IGSDKYFHAR GNYDAAKRGP GGVWAAEAIS NARENIQRFF GRGAEDSLAD QAANEWGRSG KDPNHFRPAG LPEKY. Apo-SAA has previously been used for mouse pulmonary exposures[29,30] and at the time of the experiments no mouse SAA3 existed on the market. Human serum albumin (HSA) was purchased from Sigma (#A1653, Sigma-Aldrich, Germany). Endotoxin has previously been measured to <0.03 EU/mL in HAS.[31] Isoflurane 100% w/w inhalation vapor-liquid was ISOBA VET (MSD Animal Health, UK).

2.2 | Animals, diet, and housing conditions

Female wild-type C57BL/6-Ntac (C57BL/6) mice (Taconic, Denmark) were used in the first of two pilot studies for

FIGURE 1 Mechanism of action from pulmonary exposure to atherosclerosis. The relationship between exposure to particles and effect on inflammation, acute phase response as well as on intermediary blood biomarkers, and atherosclerosis. Grey dotted box illustrates the serum amyloid A (SAA) exposure tested in this paper. End-points in bold are measured in this paper. CHO, cholesterol; HDL, high density lipoprotein; LPO, lipid peroxidation; MDA, malondialdehyde; PMN, polymorphonuclear neutrophils; SAA, serum amyloid A; VLDL/LDL, very-low density lipoprotein/low density lipoprotein
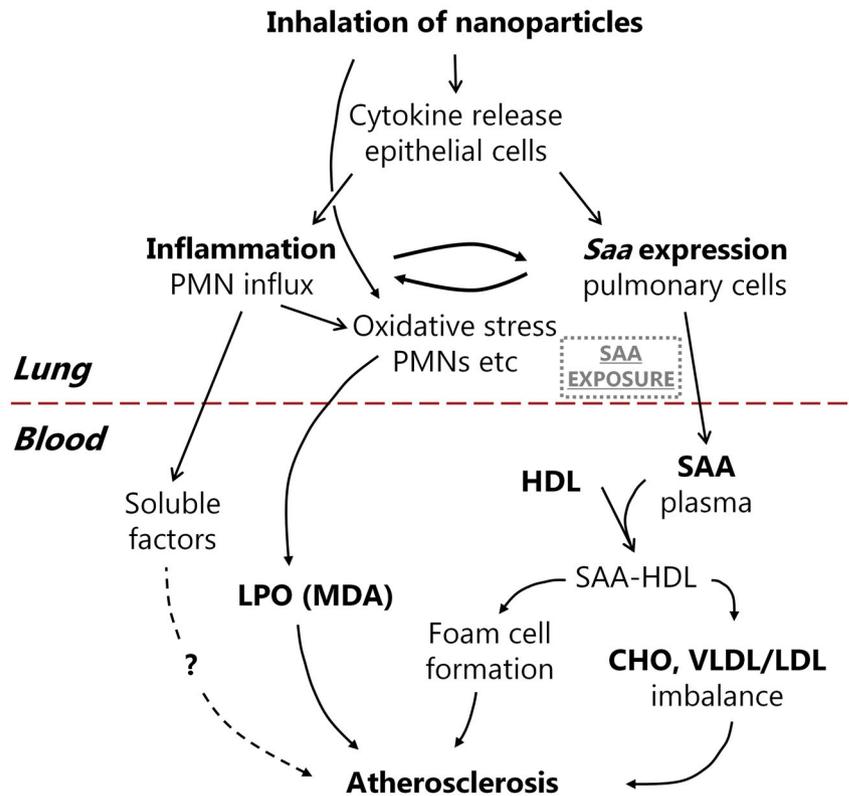
finding the optimum SAA dose-range. The mice were acclimatized for one week before the first exposure at 8 weeks of age. For the second pilot study and for the main study, female C57BL/6-Apoe$^{tm1\ Unc}$ N11 ($ApoE^{-/-}$) mice (Taconic, Denmark) were given two weeks of acclimation before the first exposure at 10 weeks of age. These studies were for detecting effects of single and repeated pulmonary SAA exposures, respectively.

All mice were randomly assigned to groups of five mice and housed in polypropylene cages (Jeluxyl HW 300/500) with sawdust bedding and enrichment, such as pinewood sticks and rodent tunnels. The cages were stored in the animal facility with a 12:12 hour light-dark cycle with controlled humidity and temperature and all cages were sanitized once a week. Mice of pilot study 1 (C57BL/6) and the chow-fed group of pilot study 2 ($ApoE^{-/-}$) had ad libitum access to regular mouse chow (Altromin no. 1324 Christian Petersen, Denmark) and tap water. The feed for the mice of pilot study 2 and the main study was switched from chow to ad libitum access to Western-type diet (21% milk fat [w/w], 0.21% cholesterol [w/w]; Open Source Diets, RD Western Diet Product # D12079B) one and two weeks prior the first exposure, respectively. The study and all animal procedures were approved by the local animal ethical committee as well as the Danish Animal Experimental Inspectorate under the Ministry of Justice (permission 2010/561-1779 and 2013-15-2934-00762).

2.3 | Study design

2.3.1 | SAA dose-finding in wild type mice (pilot study 1)

The SAA dose-range pilot study was designed to find a dose of SAA that induced low to moderate inflammation in C57BL/6 mice. In the assessment of the dose-response relationship, we exposed C57BL/6 mice to a single bolus of PBS (vehicle), 0.25, 1.0, and 4.0 µg of recombinant hApo-SAA using i.t. instillation. All mice were euthanized 24 or 72 hours after the final exposure (n = 3 mice/group) and bronchoalveolar lavage (BAL) fluid was collected. Based on the obtained result of this pilot study, we chose 2 and 6 µg for the below described $ApoE^{-/-}$ study as doses that would cause low to moderate neutrophil influx in BAL fluid (Figure 2).

2.3.2 | Single SAA exposure in ApoE$^{-/-}$ mice (pilot study 2)

The aim of this pilot study was to investigate the short-term effects of elevated pulmonary SAA on blood lipid composition, and markers of inflammation and oxidative stress in a relevant animal model for atherosclerosis.

Four groups of $ApoE^{-/-}$ mice (6 mice/group) received a single bolus i.t. instillation with vehicle (PBS), 2 or 6 µg
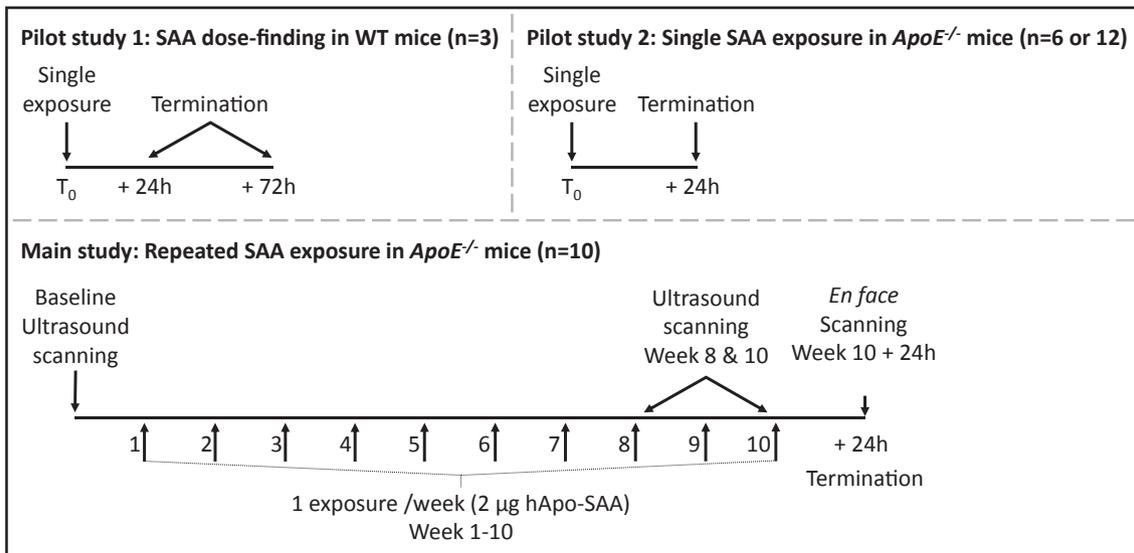
FIGURE 2 Illustration of the three studies conducted. See Materials and Methods for further details

recombinant hApo-SAA, or 6 μg HSA. From other studies, we know the level of pulmonary inflammation induced by HSA in $ApoE^{-/-}$ mice; thus, in the present study, it is regarded as a known protein-control. All mice were killed 24 hours after exposure (Figure 2).

In order to further explore observed difference between SAA and HSA, the above study was repeated in a reduced setup hereby increasing the sample size. Three groups of $ApoE^{-/-}$ mice (6 mice/group) received a single bolus i.t. instillation with vehicle (PBS), 6 μg recombinant hApo-SAA, or 6 μg HSA. Additionally, two unexposed $ApoE^{-/-}$ mice was included.

2.3.3 | Repeated SAA exposure in ApoE$^{-/-}$ mice (main study)

The purpose of this study was to investigate if 10 weeks of elevated levels of pulmonary SAA would exacerbate the progression of atherosclerotic lesions in $ApoE^{-/-}$ mice. Two groups (10 mice/group) were i.t. instilled once a week for 10 consecutive weeks with vehicle (PBS) or 2 μg hApo-SAA protein (summarized dose: 20 μg/mouse). The SAA dose used in the main study was chosen based on results from the single dose study in $ApoE^{-/-}$ mice (pilot study 2), that is, a dose resulting in a moderate pulmonary inflammation and at the same time avoiding severe neutrophilia. Six mice from each group underwent high-frequent ultrasound scanning of the aortic arch at week 0, week 8, and week 10 (immediately before euthanization). All mice were killed 24 hours after the final exposure (Figure 2).

2.3.4 | Intratracheal instillation

All mice were exposed via i.t. instillation. We have previously described the technique in details.[6,32] Briefly, the

mice were anesthetized using 3%-4% isoflurane until fully relaxed. They were transferred back down to a 50° instillation board. A diode light source was positioned on the larynx to visualize the epiglottis, trachea, and vocal cords. The tongue was gently pressed towards the lower jaw using a small spatula, and the trachea was intubated using a 24 gauge BD Insyte catheter (Ref: 381212, Becton Dickinson, Denmark) with a shortened needle. To ensure that the tube was positioned correctly in the trachea, an extremely sensitive pressure transducer was used to measure the mouse respiration as previously described.[33] Fifty microliters of solution was instilled immediately followed by 200 μL air using a 250 μL SGE glass syringe (250F-LT-GT, Micro-Lab, Denmark). After instillation, the mice were weighed and when fully conscious (within a few minutes) transferred to their cages.

2.3.5 | Bronchoalveolar lavage and isolation of organs

All mice were anesthetized by a subcutaneous injection of Hypnorm/Midazolam, (2 Water: 1 Hypnorm: 1 Midazolam [5 mg/mL]). The weight was recorded, and as previously described by Jacobsen et al[34] blood and BAL was collected. Briefly; blood was collected by cardiac puncture in an Eppendorf tube containing 36 μL K$_2$EDTA. Blood was centrifuged at 2000g, 4°C, for 5min immediately, and plasma was collected. BAL was performed by cannulating trachea using a 22 gauge needle equipped with polyurethane catheter. The lungs were flushed twice (2 × 0.8 mL/mouse) using physiological saline. Each flush consisted of one slow down and upward movement using a 1 mL disposable syringe. The total BAL fluid volume recovery was estimated to be around 80%. The BAL fluid was kept on ice (less than 1h) until it was centrifuged

at 400 *g* at 4°C for 10 minutes. and the acellular supernatant stored at −80° until use. The BAL cell pellet was resuspended in 100 μL media (HAMS F12 (GIBCO #21765) supplemented with 10% FBS). The total BAL cell count of each mouse was determined using 40 μL cell suspension in a NucleoCounter NC-100 (ChemoMetec A/S, Denmark). To prepare Cytospin slides, 40 μL cells suspension was used and centrifuged at 1000 rpm (~60 g) for 4 min. The slides containing cells from BAL fluid were stained using May-Grunwald/Giemsa co-staining. The cell composition was determined by counting 200 cells per slide by a person blinded to the exposure groups.

Tissues from the mice in the repeated dose study (main study) were harvested immediately after the BAL procedure as previously described.[35] Lungs and liver were dissected, snap frozen in liquid nitrogen and stored at −80°C. The heart and the whole aorta (from the arch to the iliac bifurcation) were carefully dissected and transferred to a Petri dish containing oxygenated ice-cold physiological phosphate solution (PSS). The heart and aorta were kept in cold PSS at 4°C for up to 4 hours until trimming was completed.

2.4 | Atherosclerotic plaque progression in the aorta

Atherosclerotic plaque progression was noninvasively investigated in $ApoE^{-/-}$ mice from the main study in real-time using ultrasound imaging and postmortem histologically by en face analysis.

2.4.1 | Ultrasound imaging of the aortic arch

High frequent ultrasound imaging of the aortic arch was used as a non-invasive method for evaluating the continuous development of atherosclerotic lesions in the aorta of $ApoE^{-/-}$ mice.[36] Mice were anesthetized with 2% isoflurane and placed in supine position on a heating pad during the scanning. Body temperature, heart rate, and respiration were closely monitored during the procedure. The fur on the chest was gently removed using a hair removal cream (Veet, Reckitt Benckiser Group plc, England) and aquasonic gel (Mærsk-Andersen, Denmark) was applied to the chest for optimal contact between the scan head and the skin. Ultrasound imaging was performed using the Vevo 770 system (VisualSonics, Canada) equipped with the 40MHz RMV-704 scan head. Imaging was performed in the long-axis view using M-mode with the scan head fixed in the VisualSonics Vevo Integrated Rail System II. To ensure reproducibility and accuracy of each scan the brachiocephalic artery was used as an anatomical landmark and scanning of the aortic arch were done at the depth of 5-6 mm. After scanning, the mouse was allowed to recover from anesthesia before being transferred back to its cage.

2.4.2 | En face analysis of the aorta

The heart and the aorta were placed in ice-cold oxygenated PSS buffer. Fat- and connective-tissue were carefully removed using micro scissors under an Olympus SZX7 stereomicroscope. The trimmed aorta was cut longitudinally from the arch to the iliac artery, and then, flatted and mounted between an objective glass and a cover slide, avoiding any overlapping tissue. Digital images of the intimal surface were obtained using an Olympus SZX7 stereomicroscope and Olympus Color View I camera. The level of aorta of atherosclerotic lesions was quantified as the percentage of plaque covering the intima surface area of the aorta and was evaluated and quantified by a person blinded to the exposure groups. Data analysis was carried out using ImageJ software.

2.5 | Plasma malondialdehyde (MDA) levels

As a marker of systemic oxidative stress, we measured the lipid peroxidation product MDA in plasma using high-performance liquid chromatography (HPLC) with fluorescence detection as previously described.[37] All analyses were run in triplicates.

2.6 | *Saa1* and *Saa3* mRNA expression in liver and lung tissue

As previously described,[38] RNA from lung (~ 20 mg) and liver (~ 20 mg) of each mice were isolated on a Maxwell 16 (Promega) using Maxwell 16 LEV simply RNA Tissue Kit (AS1280, Promega) according to the manufacturer's protocol with the following exception. RNA was eluted in 50 μL nuclease free (diethyl pyrocarbonate; DEPC) water.

Complementary DNA (cDNA) was prepared from DNAse treated RNA using Taq-Man reverse transcription reagents (Applied Biosystems, USA) according to the manufacturer's protocol. Total RNA and cDNA concentrations were measured on NanoDrop 2000c (Thermo-Fisher). The *Saa1* (Mm00656927 gi) and *Saa3* gene expression were determined using real-time polymerase chain reaction (RT-PCR) with 18S RNA as reference gene as previously described.[21] Briefly, each sample was run in triplicate on a ViiA7 sequence detector (Applied Biosystems, USA). For Saa1 (Mm00656927 gi) pre-developed TaqMan reaction kit (Applied Biosystems, USA) were used. The sequence of the *Saa3* primers and probe were *Saa3* forward: 5′ GCC TGG GCT GCT AAA GTC AT 3′, Saa3 reverse: 5′ TGC TCC ATG TCC CGT GAA C 3′, and *Saa3* probe: 5′ FAM TCT GAA CAG CCT CTC TGG CAT CGC T-TAMRA 3′. In all assays, TaqMan pre-developed master mix (Applied

Pilot study 1	Vehicle	0.25 µg SAA	1 µg SAA	4 µg SAA
Total cells	58.0 ± 4.8	35.4 ± 2.5	51.1 ± 11.7	87.7 ± 6.1
Neutrophils	0.4 ± 0.4	0.4 ± 0.2	0.7 ± 0.3	$18.5 \pm 4.1^{**}$
Macrophage	49.0 ± 4.3	32.7 ± 2.4	45.1 ± 10.3	58.1 ± 8.0
Eosinophils	0.1 ± 0.1	0.0 ± 0.0	0.0 ± 0.0	0.4 ± 0.4
Lymphocytes	0.1 ± 0.1	0.1 ± 0.1	0.2 ± 0.1	0.4 ± 0.2
Epithelial	8.4 ± 3.1	2.4 ± 0.5	5.1 ± 1.1	10.3 ± 4.1
BAL fluid cell number and distribution 72 h post a single exposure to SAA				
Total cells	43.3 ± 15.8	50.1 ± 2.6	41.6 ± 3.9	48.8 ± 6.5
Neutrophils	0.0 ± 0.0	0.2 ± 0.1	0.2 ± 0.1	0.7 ± 0.3
Macrophage	38.1 ± 14.1	43.8 ± 2.1	34.0 ± 0.9	43.3 ± 6.1
Eosinophils	0.02 ± 0.02	0.2 ± 0.08	0.06 ± 0.06	0.0 ± 0.0
Lymphocytes	0.2 ± 0.1	0.5 ± 0.3	0.3 ± 0.08	0.7 ± 0.2
Epithelial	5.0 ± 2.3	5.4 ± 1.5	7.0 ± 3.4	4.2 ± 0.5

Note: Results are presented as mean $\pm$ SEM (N = 3). Asterisks refer to statistical significance $^{**}P < .01$ compared to the vehicle control. Statistical analyses were performed using one-way ANOVA with Tukey's post hoc test.

Biosystems, USA) was used. The relative expression of the target gene was calculated by the comparative (normalization) method $2^{-\Delta Ct}$.[39]

All mRNA samples delivered results within the quantifiable range of the PCR defined by the validation experiments. No template controls (without cDNA/RNA) and no reverse transcriptase control (-RT, with RNA and very small amounts of DNA), where RNA had not been converted to cDNA, were included. The analysis was performed on a single 384 well plate, that is, no day to day variation.

2.7 | Plasma levels of serum amyloid A3 (SAA3)

For specific assessment of circulating SAA3 levels, we used a mouse SAA3 ELISA kit with a detection limit of 0.08 µg/mL (Cat.no. EZMSAA3-12K, Merck Millipore, Denmark). All measurements were carried out on plasma samples from $ApoE^{-/-}$ mice according to the manufacturer's instructions. The SAA3 ELISA kit does not detect a response in samples spiked with human Apo-SAA, indicating that the SAA3 in plasma samples from mice has endogenous origin.[22] We did not measure human SAA in plasma as to the best of our knowledge; no species specific and validated assay exists for this protein.

2.8 | Plasma cholesterol and lipoprotein

The plasma levels of HDL, low-density lipoproteins + very low-density lipoproteins (LDL + VLDL), and total cholesterol were measured using an enzymatic kit (EnzyChrom HDL and LDL/VLDL Assay Kit, BioAssay Systems LLC, USA) according to manufacturer's instructions. The assay does not discriminate between LDL and VLDL; thus, LDL + VLDL are the sum of the two. The plate was read at 340 nm using an Epoch Microplate Spectrophotometer (BioTek, Germany).

2.9 | Statistics

Vehicle and SAA exposed mice were analyzed by one-way ANOVA with Tukey's post hoc test for the dose-finding study in wild-type C57BL/6 mice (pilot study 1) and single dose in $ApoE^{-/-}$ (pilot study 2) and by Student's *t* test for the repeated dose study in $ApoE^{-/-}$ (main study). All results from unexposed mice on normal chow diet are shown without a statistical assessment as all other groups (vehicle controls or SAA exposed) were on Western-type diet. The following BAL fluid cell counts displayed inhomogeneity of variance and were logarithm transformed before the statistical analysis: Single dose in $ApoE^{-/-}$ (pilot study 2): Total BAL fluid cells, neutrophils, eosinophils, and lymphocytes. The pilot study 2 was repeated for the 6µg SAA and HSA groups, and the results were pooled for the statistical analysis (ie, the results from the low-dose SAA groups are not included in the statistical analysis, although they are reported in the tables). Repeated dose study in $ApoE^{-/-}$ (main study): Total BAL fluid cells, lymphocytes, neutrophils, and eosinophils. In addition, the results of MDA levels (pilot study 2) and LDL-VLDL and total cholesterol also displayed inhomogeneity of variance and were logarithm transformed before the statistical analysis. However, for consistency, we have reported the P-values from the parametric analysis, which did not differ as compared to Student's *t* test with unequal variance between

TABLE 2 BAL fluid cell number ($\times 10^3$) and distribution 24-hour post a single exposure in $ApoE^{-/-}$ mice

Pilot study 2	Vehicle	2µg SAA	6µg SAA	6µg HSA
Total cells	55.3 ± 5.5	38.9 ± 7.9	101.5 ± 15.8	61.8 ± 9.7
Neutrophils	5.8 ± 3.0	2.3 ± 1.7	56.3 ± 9.7***	10.2 ± 3.7###
Macrophage	43.1 ± 4.1	33.3 ± 8.2	40.2 ± 6.7	47.2 ± 9.1
Eosinophils	1.8 ± 1.0	0.2 ± 0.2	0.6 ± 0.2	0.2 ± 0.1
Lymphocytes	0.6 ± 0.1	0.3 ± 0.1	1.3 ± 0.2	0.7 ± 0.2
Epithelial	6.3 ± 0.9	4.6 ± 1.3	3.1 ± 0.7	5.1 ± 0.9

Note: All cells are listed in actual numbers /1000. Values are given as mean ± SEM of 12, 6, 12, and 11 animals for total cells and 11, 5, 12, and 10 for differential cell counts for vehicle, 2 µg SAA, 6 µg SAA, and 6 µg HSA, respectively. Asterisks refer to statistical significance ***$P < .001$ compared to the vehicle control and ###$P < .001$ compared to 6 µg SAA. Statistical analyses were performed using one-way ANOVA with Tukey's post hoc test.

groups. All results are reported as mean ± standard error of the mean (SEM). As several of the data sets displayed inhomogeneity of variance and were logarithm transformed before the statistical analysis, fold induction may be different from that calculated directly from the tables and figures. Especially, the fold-ratios from raw data and log-transformed differed by more than 20% in datasets of neutrophils in BALF (pilot study 2) and MDA levels in plasma (Main study). For these datasets we report both the raw and log-transformed fold-ratios. Statistical significance was accepted at 5% level. All P-values refer to post hoc tests. The statistical analysis was carried out in Statistica for Windows version 5.5 (StatSoft, USA) and GraphPad Prism version 5.00 for Windows (GraphPad Software, USA).

3 | RESULTS

3.1 | Bodyweight

There were no differences with respect to the weight between the groups of mice exposed to vehicle or the exposures (hApoSAA or HSA) before or after the experiment in any of the three studies (Pilot study 1, 2 and main study)(data not shown).

3.2 | Bronchoalveolar lavage fluid cells

3.2.1 | Dose-finding in wild type mice (pilot study 1)

A single i.t. instillation with 4 µg SAA (high dose group) in C57BL/6 mice significantly increased the number of neutrophils (44.7-fold, CI: 24.5-64.9, $P < .01$) 24 hours after exposure compared with controls (Table 1). The two lower SAA doses (0.25 and 1 µg) did not cause neutrophil influx compared to vehicle exposed. Although about 50% increase in total cells was observed, we did not find statistically significant differences in the number of total cells, macrophages, lymphocytes, eosinophils, or epithelial cells between SAA

and vehicle exposed mice 24 hours after last exposure. The changes observed 24 hours after exposure to 4 µg SAA were not present 72 hours after exposure (Table 1).

3.2.2 | Single dose study in ApoE$^{-/-}$ mice (pilot study 2)

I.t. instillation with a single dose of 6 µg SAA in $ApoE^{-/-}$ mice increased the number of neutrophils (56.3×10^3 vs 5.8×10^3 cells) in BAL fluid, corresponding to 9.7-fold increase using untransformed results and 19.7-fold on log-transformed results (95% CI: 5.8-66.5, $P < .001$). The i.t. instillation with a single dose of 6 µg HSA did not increase the number of neutrophils (Table 2). Moreover, SAA produced a larger influx of neutrophils in BALF as compared with HSA (7.8-fold, 95% CI: 2.2-27.1, $P < .001$). The total cell number was also increased in SAA exposed mice as compared to controls (1.7-fold, 95% CI: 1.0 - 2.8, $P < .05$). As also observed in pilot study 1, exposure to SAA did not significantly affect the numbers of macrophages, eosinophils, lymphocytes or epithelial cells. Taken together these results suggest that a strong inflammatory pulmonary response is observed from 4 µg SAA exposure. We chose to use a somewhat lower dose of 2 µg SAA for the repeated dose study because we have previously observed an accumulation of BAL cells following repeated vehicle (2% mouse serum) instillations.[40] This dose (2 µg SAA) has previously been used in repeated exposures to induce netrophil influx in mice.[29] In comparison, it has been shown that wild-type mice had ~0.3 µg SAA3 in BAL fluid following a single instillation with MWCNT,[21] whereas plasma SAA3 levels of 3.5 ug/mL were found in following pulmonary exposure to MWCNT.[23]

3.2.3 | Repeated dose study in ApoE$^{-/-}$ mice (main study)

I.t. instillation of 2 µg SAA once weekly for 10 weeks resulted in increased numbers of total cells (7.5-fold, 95% CI: 5.9-9.1 fold, $P < .001$), neutrophils (625-fold, 95% CI:

476-774 fold, $P < .001$), macrophages (1.5-fold, 95% CI: 1.01-2.0 fold, $P < .05$), eosinophils (8.4-fold, 95% CI: 3.8-12.9 fold, $P < .01$), and lymphocytes (22.8-fold, 95% CI: 8.8-36.7 fold, $P < .01$)in BAL fluid of the mice exposure to SAA as compared to controls (Table 3).

3.3 | Atherosclerotic plaque progression

3.3.1 | En face measurement of aortic lesions (main study)

Repeated pulmonary exposure to SAA significantly increased the percentage of atherosclerotic lesions in the aorta of $ApoE^{-/-}$ mice (1.5-fold, 95% CI: 1.11-1.93, $P < .05$) compared to the vehicle exposed group (Figure 3). The chow fed $ApoE^{-/-}$ mice that did not receive any exposure had substantially lower plaque area compared to vehicle (PBS) exposed $ApoE^{-/-}$ mice on Western-type diet, showing a large combined effect of the

TABLE 3 BAL fluid cell number ($\times 10^3$) and distribution 24 h post exposure (10 weeks of exposure $ApoE^{-/-}$ mice)

Main study	Vehicle	SAA
Total cells	41.5 ± 4.6	310.0 ± 30.0***
Neutrophils	0.4 ± 0.2	221.9 ± 23.8***
Macrophage	36.0 ± 4.2	53.5 ± 6.7*
Eosinophils	0.6 ± 0.2	5.3 ± 1.3**
Lymphocytes	0.9 ± 0.3	22.4 ± 6.1**
Epithelial	3.2 ± 0.5	6.5 ± 2.0

Note: Mice were administered 2 µg per i.t. instillation (Total dose = 20 µg/ mouse). Data are presented as Mean ± SEM of N = 10. Asterisks denote *$P < .05$, **$P < .01$, ***$P < .001$ cells influx in SAA exposed group compared to vehicle group, respectively. Statistical analyses were carried out using Student *t* test.

diet and vehicle exposure (5.6-fold, CI: 3.2-8.0, $P < .001$) on plaque progression in the aorta (Figure 3).

3.3.2 | Ultrasound scanning of the aortic arch (main study)

Ultrasound scanning of the aortic arch showed a time-dependent increase in the inner ($P < .001$) and outer ($P < .001$) wall thickness, whereas there was no statistically significant difference in the lumen diameter in $ApoE^{-/-}$ mice. The exposure to SAA did not affect the inner- or outer wall thickness or the lumen diameter of the aorta after 8 or 10 weeks of exposure (Figure 4).

3.4 | *Saa1* and *Saa3* mRNA expression in liver and lung tissue

Repeated i.t instillations with SAA significantly increased the mRNA expression of *Saa1* in the liver (2.4-fold CI: 1.15-3.73, $P < .05$) and *Saa3* expression in lung tissue (196-fold CI: 131-261, $P < .001$) compared to vehicle exposed $ApoE^{-/-}$ mice 24 hours after the last of 10 exposures (Figure 5).

3.5 | SAA3 levels in plasma

Twenty-four hours postexposure to a single dose of SAA, there was no difference in SAA3 plasma levels between SAA exposed $ApoE^{-/-}$ mice and controls (Figure 6). Moreover, HSA did not significantly increase the plasma levels of SAA3. However, $ApoE^{-/-}$ mice exposed to repeated SAA i.t. instillations had significantly more endogenous SAA3 in plasma (1.8-fold, CI: 1.3-2.3, $P < .01$) compared to vehicle exposed group (Figure 6).
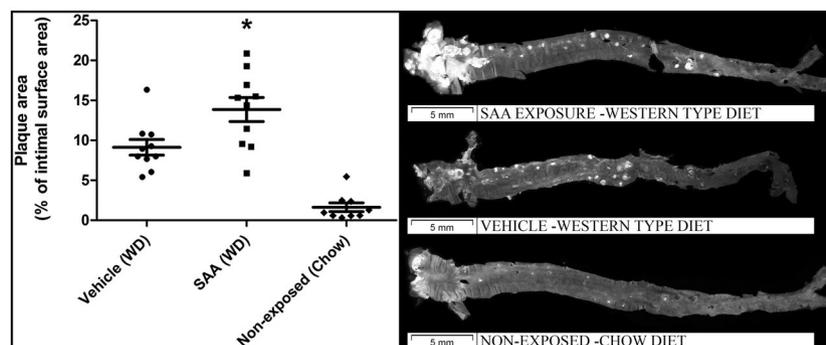

FIGURE 3 Atherosclerotic lesions in aorta. Aorta plaque area (%) in $ApoE^{-/-}$ mice after 10 i.t. instillations with PBS (circles) or serum amyloid A (SAA) (summarized dose: 20 µg, squares) both groups of mice were fed Western-type Diet (WD) (n = 10). The third group of $ApoE^{-/-}$ mice fed standard mouse chow diet and received no exposure (diamonds) (n = 10). Asterisk refer to statistical significance *$P < .05$ between vehicle and SAA exposure in mice fed Western-type diet (Student's *t* test). Unexposed mice on chow diet were not included in the statistical analysis. Representative examples of en face scanning images of aortas from mice showing plaque area just above the group mean. The shown examples had 15.4% (SAA exposure), 10.8% (Vehicle), and 2.5% (Non-exposed) aorta plaque area
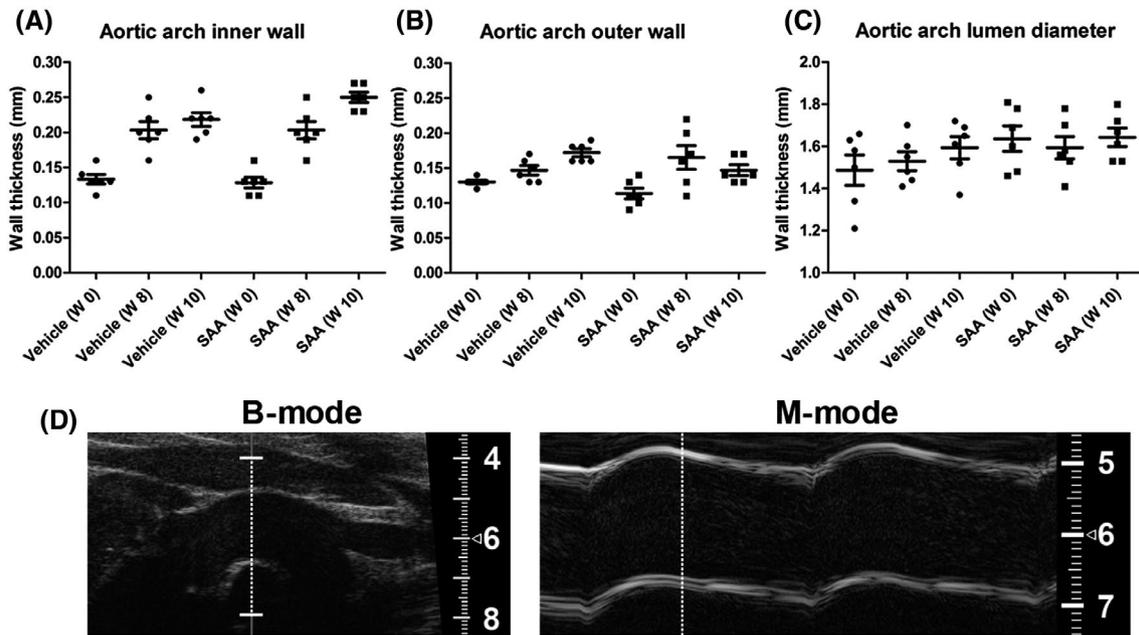
FIGURE 4 Ultrasound imaging of the aorta arch. Ultrasound scanning and imaging of the aortic arch was performed on live *ApoE*⁻/⁻ mice in real-time at baseline (W 0), 8 weeks (W 8) and 10 weeks (W 10) of exposure. A, Measurements of the inner wall thickness. B, Measurements of the outer wall thickness. C, The aortic arch lumen diameter. D, An example of an ultrasound scanning image from an *ApoE*⁻/⁻ mouse following 10 weeks of SAA exposure is displayed in B-mode and M-mode view. In B-mode, the aortic arch and the brachiocephalic artery (the anatomic landmarked used) is clearly visible. The vertical dotted line indicates the scanning site for the single ultrasound beam in the high-resolution M-mode. The M-mode image shows the aortic arch with the outer wall (top), the lumen and the inner wall (bottom). The vertical dotted line located about 1/10th into the diastole illustrates the measuring point used. Data are presented as mean $\pm$ SEM. Each data point represents an individual mouse (n = 6). Statistical analyses were carried out using repeated measurement ANOVA with Tukey's post hoc test and $P < .05$ was considered statistically significant, however, no statistically significant changes between vehicle and SAA exposed mice were observed
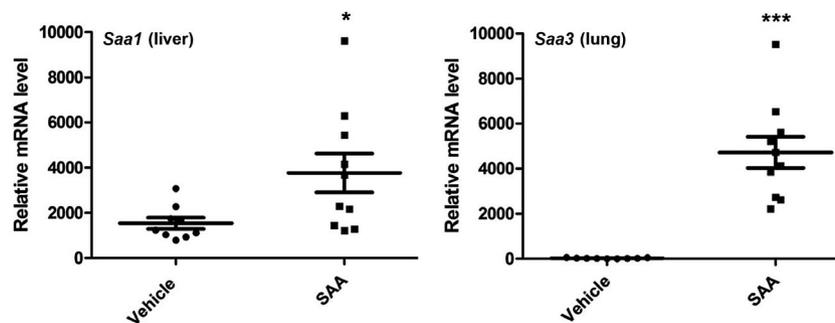

FIGURE 5 Acute phase response in liver and lung. Serum amyloid A1 (*Saa1*) mRNA levels in liver tissues (left) and *Saa3* mRNA levels in lung tissues (right) from *ApoE*⁻/⁻ mice after i.t. instillations with vehicle (PBS) or serum amyloid A (SAA). Mice were exposed to repeated instillation with vehicle or SAA 2 µg (summarized dose: 20 µg). Gene expression mRNA levels were measured 24 h after the last exposure. Each data point represents an individual mouse (n = 10). *$P < .05$ and ***$P < .001$ compared to the vehicle exposed group (Student's t test)

3.6 | Lipid composition in plasma

HDL, LDL + VLDL, and total plasma cholesterol were measured in plasma of *ApoE*⁻/⁻ mice. Repeated pulmonary exposure to SAA significantly decreased the plasma levels of LDL + VLDL (0.89-fold, CI: 0.87-0.91, $P < .01$) and total cholesterol (0.91-fold, CI: 0.85-0.96, $P < .01$) as compared to vehicle exposed mice (Table 4). The HDL concentrations were below the detection limit (5 mg/dL) of the assay.

3.7 | MDA levels in plasma

There was no significant effect of a single i.t. instillation of SAA on the plasma levels of MDA in *ApoE*⁻/⁻ mice (Figure 7). Mice exposed to a single bolus dose of 6 µg of HSA had significantly lower plasma levels of MDA (0.88-fold, CI: 0.81-0.95, $P < .001$) than mice exposed to 6 µg SAA. Repeated i.t. instillations in *ApoE*⁻/⁻ mice (total dose of 20 µg SAA) increased the plasma MDA

levels 24 hours after last exposure (1.45 vs 0.97 nmol/mL in the vehicle exposed group) (Figure 7), corresponding to 1.50-fold increase using untransformed results and 1.14-fold on log-transformed results (1.14-fold, CI: 1.05-1.24, $P < .001$). Unexposed $ApoE^{-/-}$ mice fed regular chow diet had higher plasma MDA levels as compared to vehicle

exposed mice on a Western-type diet (1.71-fold, CI: 1.50-1.93, $P < .001$) (Figure 7). This unexpected observation is most likely due to a high content of MDA in the standard chow diet (8.8 nmol/g) compared to the Western-type diet (0.3 nmol/g); a 29-fold difference.

TABLE 4 Plasma Cholesterol 24 h postexposure (10 weeks of exposure $ApoE^{-/-}$ mice)

Main study	Vehicle	SAA
HDL (mg/dL)	<5 ± 0	<5 ± 0
LDL + VLDL (mg/dL)	425 ± 25	325 ± 11**
Total cholesterol (mg/dL)	550 ± 33	434 ± 15**

Note: Plasma cholesterol from $ApoE^{-/-}$ mice (n = 10) after 10 weekly i.t. instillations of vehicle (PBS) or SAA (Summarized dose = 20 μg/mouse). Results are presented as the mean ± SEM. Asterisks refer to statistical significance **$P < .01$ compared to the vehicle exposed group. Statistical analyses were carried out using Student *t* test.

4 | DISCUSSION

Here we show that multiple SAA i.t. instillations caused lung inflammation and accelerated atherosclerotic plaque progression in hyperlipidemic $ApoE^{-/-}$ mice. The plaque area in the aorta increased 1.5-fold scored by histopathological assessment using en face analysis. However, using ultrasound imaging, we only observed a marginal increased effect of SAA exposure on the inner arch wall thickness. This finding could be due to regional differences in the distribution of atherosclerotic lesions in the aorta arch.
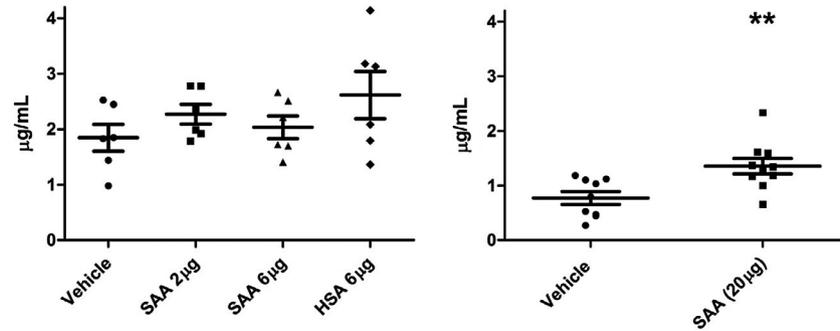

FIGURE 6 Serum amyloid A3 (SAA3) levels in plasma following single or repeated SAA exposures. Plasma SAA3 from $ApoE^{-/-}$ mice after i.t. instillations with vehicle (PBS) or serum amyloid A (SAA). Mice were exposed to single instillation with vehicle, SAA 2 μg, SAA 6 μg, or HSA 6 μg (left) or repeated i.t. instillations with vehicle or SAA (summarized dose: 20 μg) (right). SAA3 plasma levels were measured 24 h after last exposure. Each data point represents an individual mouse (n = 10). **$P < .01$ compared to the vehicle exposed group (Student's *t*-test)
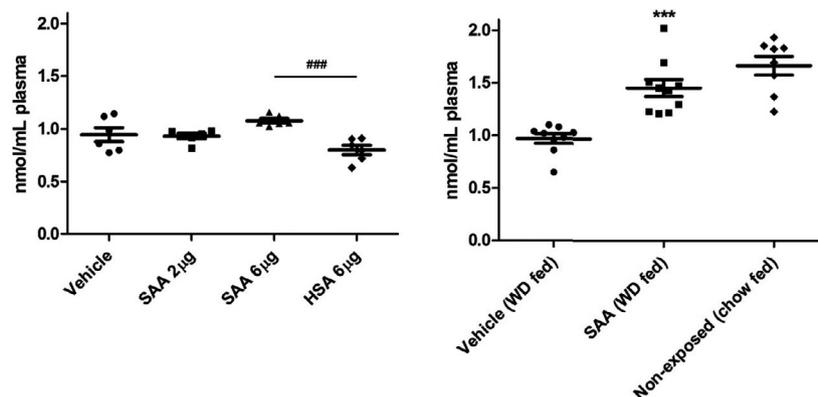

FIGURE 7 Plasma level of Malondialdehyde (MDA) following single or repeated SAA exposures. MDA as a measure of systemic lipid peroxidation was assessed in plasma of $ApoE^{-/-}$ mice after i.t. instillation of serum amyloid A (SAA). Left: MDA plasma levels from mice fed a chow diet and instilled with a single dose of vehicle (PBS), 2 μg SAA, 6 μg SAA, or 6 μg human serum albumin (HSA) (n = 6). Right: MDA plasma levels from mice instilled with vehicle (PBS) or SAA (20 μg) weekly for 10 weeks and a group of mice on chow diet that did not receive any exposure (n = 10). Data are presented as mean ± SEM, and each data point represents an individual mouse. Asterisks denote ***$P < .001$ compared to the vehicle exposed group using Student's *t* test. Hashtags denote ###$P < .001$ compared to the 6 μg SAA group using ANOVA with Tukey's post hoc test

Ultrasound imaging is performed on a specific and narrow cross section of the aortic arch, whereas the en face method is performed on the whole aorta from the ascending aorta to the iliac bifurcation. Pulmonary exposures to nanoparticles and fibers have previously been shown to accelerate atherosclerosis in $ApoE^{-/-}$ and $Ldlr^{-/-}$.[6,8,9,41] The mechanistic linkage between exposure to particles and cardiovascular effects is typically considered to be mediated by inflammatory signaling, APR and oxidative stress[10] (Figure 1). It has previously been shown that a systemic Lenti-SAA virus mediated increase in SAA promoted plaque formation and that SAA and macrophages accumulated and colocalized in the lesions. The macrophages attracted to the early atheroma rapidly phagocytize SAA-HDL complexes, increasing the volume of the plaque.[25] We expect a similar chain-of-events to be the cause of the increased plaque progression observed in the present study as it has been shown that nanomaterial-induced lung $Saa3$ levels correlate with SAA3 blood levels.[14,23] This suggests that pulmonary SAA3 reach systemic circulation.

SAA is also strong neutrophilic chemoattractant[42] and in agreement with this, i.t. instillation of 4 or 6 μg SAA in the lungs of wild-type (C57BL/6) or $ApoE^{-/-}$ mice, respectively, caused a significant and comparable large influx of neutrophils in BAL fluid after 24 hours. The number of neutrophils in BAL fluid subsided to baseline after 72 hours in wild-type mice, which is similar to the kinetics described in other studies.[29,43] Interestingly, although an exposure of 2 μg SAA only caused a non-significant 1.5-fold increase to 2300 neutrophils in $ApoE^{-/-}$ mice (Table 2), and the elevated SAA levels subsided rapidly in wild-type mice, the inflammation was strongly amplified during the 10 weeks of exposure (1 exposure/week). At termination the influx had increased to 221 900 neutrophils. Although, this is a very large increase, and a strong inflammation, it is comparable to, for example, the neutrophil influx at 1 day after a single it instillation of 54 μg (2.8 mg/kg) of carbon black Printex 90[44] or 3 days post 6 μg (0.3 mg/kg) i.t. instillation of ZnO nanoparticles.[32] We observed a significant increase in BAL eosinophils and lymphocytes (combined 8.9%) following the ten SAA exposure (Table 3). Inductions of these levels are common following exposures to nanoparticles in general, but especially exposures to nanofibers like carbon nanotubes,[45] cellulose,[46] or TiO_2 tubes[47] induce strong eosinophilic responses.

Oxidative stress is another suggested key mechanism of particle-induced atherosclerosis. Lipid peroxidation in plasma is associated with foam cell formation and development of atherosclerotic plaques in $ApoE^{-/-}$ mice.[48,49] Both oxidized LDL and MDA are present in foam cells in the artery wall, emphasizing the importance of lipid peroxidation in atherosclerosis.[49,50] As evident from our results, ingestion of high levels of MDA, as present in chow diet, may increase MDA plasma levels (Figure 7), but this did not have an effect

on plaque progression (Figure 3). In the present study, we detected a 1.14-fold increase in the plasma concentration of MDA in the SAA-exposed mice (Figure 7). Interestingly, previous observations have shown that exposure to nanoparticles increased the APR and systemic levels of SAA.[11,35] In turn, elevated levels of SAA facilitates the displacement of the apoA-I subunit in HDL,[51] forming SAA-HDL. This decreases the anti-oxidant capacity of HDL and results in increased oxidation of lipoproteins, and accelerates atherosclerosis in LDLr knockout mice.[52] This chain of events has been shown to be attenuated by administration of apoA-I subunit mimics.[53,54] It underlines the importance of HDL functionality and the SAA-HDL complex in oxidative stress and atherosclerosis.[52] We did not find an effect on HDL plasma levels (below detection limit) after 10 weeks of SAA exposure. However, we did find that 10 weeks of pulmonary exposure to SAA caused a statistically significant decrease in the plasma LDL + VLDL and total cholesterol concentrations (both 0.9-fold; Table 4). A decrease in plasma cholesterol and increased plasma SAA suggest that cholesterol is detained in macrophages or foam cells in the arterial wall.[28,49] This is well in line with Lee et al, and Saber et al, who have hypothesized that during an APR the increased level of SAA-HDL inhibits the reverse cholesterol transport and facilitates the accumulation of cholesterol in the peripheral macrophages that become lipid-laden and increase the risk of foam cell formation in the artery wall.[11,28]

In the present study, we observed that the major hepatic acute phase gene $Saa1$ was modestly increased in the liver (2.4-fold) whereas pulmonary $Saa3$ was strongly induced (196-fold) after repeated i.t. instillations of SAA. The increased expression translated to a 1.8-fold increase of SAA3 in plasma. The elevated plasma levels is similar to that observed following a single exposure to 54 or 162 μg/mouse of graphene oxide[35] or 54 μg/mouse of short or long MWCNT, but much less than observed following 162 μg of the same MWCNTs.[14] Although the human recombinant Apo-SAA protein shares 74%-80% sequence identity with mouse SAA3 (the closest homolog in mouse) when aligned in the protein-protein Blast at NCBI (data not shown), the Apo-SAA is not recognized by the SAA3 ELISA.[22] The elevated concentration of SAA3 in plasma must originate from the endogenous production in the lungs as indicated by the large increase in pulmonary $Saa3$ expression, although other sources may also contribute to a lesser extent.

SAA3 has only recently been suggested as a pulmonary driver of APR, but most studies have investigated isoforms SAA1 and SAA2 in mice. We measure a modest increase in plasma levels of about 1-2 μg/mL of SAA3 (not including SAA1 and SAA2). Thompson and co-workers showed that a single injection in $ApoE^{-/-}$ with an adenoviral vector encoding human SAA1 caused a rapid increase in plasma SAA to ~27 μg/mL (day 3), which decreased after a week

to ~13 µg/mL and further almost to baseline following 2 weeks post injection. This brief but strong SAA induction caused an increase in plaque surface area to ~3.5% vs ~0.5% in controls (null viral vector) at 16 weeks postexposure.[26] Using multiple injections, the SAA levels were continuously kept elevated between 20-30 µg/mL resulting in a plaque surface area of ~5.7% (exposed) vs ~2.3% (controls) indicating the multiple handlings/injections significantly increased plaque area for both groups. There was no difference in both experiments between injections of control adenoviral vector or saline. The added effect of very high SAA levels was limited (~0.4%).[26] A review of studies with pulmonary exposure to particles showed a mean increase in atherosclerosis of 1.67-fold (CI: 1.26-2.09) between exposed and unexposed groups of animals.[8] These observations suggest that the effect of increased SAA on atherosclerosis may occur within a small dynamic range and reach a plateau at relatively low SAA plasma concentrations; including and not far above the concentrations observed following exposure to nanoparticles[11,14] and detected in this study.

As illustrated in Figure 1, our results support a very strong local pulmonary inflammation following SAA exposure. This may lead to smaller but likely biologically significant downstream effects on plasma SAA3, lipid peroxidation, cholesterol imbalance, and ultimately plaque progression. De Beer and co-workers found that disrupting SAA1/2 did not have an effect on plaque progression in $ApoE^{-/-}$ mice fed Western-type diet. It may be that results would have been different if they also had considered disrupting isoforms SAA3/4 (the latter being constitutively expressed), and it also highlights the importance of other mechanisms and pathways in atherosclerosis.[55] This is supported by the fact that inhalation of concentrated air pollution particles is associated with atherosclerosis but often not to inflammation (reviewed in Ref. 8) leading to some skepticism toward the importance of neutrophils as the link between inhalation of particles and atherosclerosis.[41] It should be noted that inhalation studies with concentrated air pollution particles are typically conducted using much lower concentrations than used in nanoparticle exposure studies, and that these exposures result in low or no inflammation but in similar or stronger effects on atherosclerosis.[8] Thus, several pathways/mechanisms are at play from inhalation of particulate matter to the development of visual plaques in arteries.

In conclusion, the present study demonstrates that repeated pulmonary i.t. instillation of SAA induces plaque progression in $ApoE^{-/-}$ mice, accompanied by a large endogenous pulmonary APR and inflammation. The results indicate the importance of the pulmonary SAA in particle-induced plaque progression and the results support previously hypothesized mechanisms like oxidative stress pathways and cholesterol sequestering.

CONFLICT OF INTEREST

The authors explicitly declare no conflict of interest in connection with this article.

AUTHOR CONTRIBUTIONS

D.V. Christophersen, H. Wallin, N.R. Jacobsen, P. Møller, S. Loft, and U. Vogel contributed to the idea and design of the study. D.V. Christophersen and N.R. Jacobsen performed the animal experiments. D.V. Christophersen performed experiments on ultrasound scanning assisted and supervised by M.B. Thomsen. D.V. Christophersen performed the experiments on plaque progression, J. Lykkesfeldt analyzed the MDA levels. D.V. Christophersen, N.R. Jacobsen, and H. Wallin performed the cholesterol and SAA3 measurements. D.V. Christophersen wrote the draft manuscript, which was critically revised by N.R. Jacobsen and P. Møller. All authors have read, commented, and approved the final manuscript.

ORCID

Nicklas Raun Jacobsen https://orcid.org/0000-0002-2504-2229

REFERENCES

1. World Health Organization. *The 10 Leading Causes of Death By Broad Income Group (2008)*. WHO. 2011.
2. Lim SS, Vos T, Flaxman AD, et al. A comparative risk assessment of burden of disease and injury attributable to 67 risk factors and risk factor clusters in 21 regions, 1990–2010: a systematic analysis for the Global Burden of Disease Study 2010. *Lancet*. 2012;380(9859):2224-2260.
3. Piedrahita JA, Zhang SH, Hagaman JR, Oliver PM, Maeda N. Generation of mice carrying a mutant apolipoprotein E gene inactivated by gene targeting in embryonic stem cells. *Proc Natl Acad Sci USA*. 1992;89(10):4471-4475.
4. Ishibashi S, Brown MS, Goldstein JL, Gerard RD, Hammer RE, Herz J. Hypercholesterolemia in low density lipoprotein receptor knockout mice and its reversal by adenovirus-mediated gene delivery. *J Clin Investig*. 1993;92(2):883-893.
5. Moghadasian MH, McManus BM, Nguyen LB, et al. Pathophysiology of apolipoprotein E deficiency in mice: relevance to apo E-related disorders in humans. *FASEB J*. 2001;15(14):2623-2630.
6. Mikkelsen L, Sheykhzade M, Jensen KA, et al. Modest effect on plaque progression and vasodilatory function in atherosclerosis-prone mice exposed to nanosized TiO(2). *Part Fibre Toxicol*. 2011;8:32.
7. Miller MR, McLean SG, Duffin R, et al. Diesel exhaust particulate increases the size and complexity of lesions in atherosclerotic mice. *Part Fibre Toxicol*. 2013;10:61.

8. Moller P, Christophersen DV, Jacobsen NR, et al. Atherosclerosis and vasomotor dysfunction in arteries of animals after exposure to combustion-derived particulate matter or nanomaterials. *Crit Rev Toxicol*. 2016;46(5):437-476.

9. Moller P, Mikkelsen L, Vesterdal LK, et al. Hazard identification of particulate matter on vasomotor dysfunction and progression of atherosclerosis. *Crit Rev Toxicol*. 2011;41(4):339-368.

10. Stone V, Miller MR, Clift MJD, et al. Nanomaterials versus ambient ultrafine particles: an opportunity to exchange toxicology knowledge. *Environ Health Perspect*. 2017;125(10):106002.

11. Saber AT, Jacobsen NR, Jackson P, et al. Particle-induced pulmonary acute phase response may be the causal link between particle inhalation and cardiovascular disease. *Wiley Interdisc Rev Nanomed Nanobiotechnol*. 2014;6(6):517-531.

12. Gabay C, Kushner I. Acute-phase proteins and other systemic responses to inflammation. *N Engl J Med*. 1999;340(6):448-454.

13. Meek RL, Eriksen N, Benditt EP. Murine serum amyloid A3 is a high density apolipoprotein and is secreted by macrophages. *Proc Natl Acad Sci U S A*. 1992;89(17):7949-7952.

14. Poulsen SS, Saber AT, Mortensen A, et al. Changes in cholesterol homeostasis and acute phase response link pulmonary exposure to multi-walled carbon nanotubes to risk of cardiovascular disease. *Toxicol Appl Pharmacol*. 2015;283(3):210-222.

15. Benditt EP, Meek RL. Expression of the third member of the serum amyloid A gene family in mouse adipocytes. *J Exp Med*. 1989;169(5):1841-1846.

16. Sellar GC, Oghene K, Boyle S, Bickmore WA, Whitehead AS. Organization of the region encompassing the human serum amyloid A (SAA) gene family on chromosome 11p15.1. *Genomics*. 1994;23(2):492-495.

17. Deguchi A, Tomita T, Omori T, et al. Serum amyloid A3 binds MD-2 to activate p38 and NF-kappaB pathways in a MyD88-dependent manner. *Journal of Immunology*. 2013;191(4):1856-1864.

18. Uhlar CM, Whitehead AS. Serum amyloid A, the major vertebrate acute-phase reactant. *Eur J Biochem*. 1999;265(2):501-523.

19. Bourdon JA, Halappanavar S, Saber AT, et al. Hepatic and pulmonary toxicogenomic profiles in mice intratracheally instilled with carbon black nanoparticles reveal pulmonary inflammation, acute phase response, and alterations in lipid homeostasis. *Toxicol Sci*. 2012;127(2):474-484.

20. Halappanavar S, Saber AT, Decan N, et al. Transcriptional profiling identifies physicochemical properties of nanomaterials that are determinants of the in vivo pulmonary response. *Environ Mol Mutagen*. 2015;56(2):245-264.

21. Saber AT, Lamson JS, Jacobsen NR, et al. Particle-induced pulmonary acute phase response correlates with neutrophil influx linking inhaled particles and cardiovascular risk. *PLoS One*. 2013;8(7):e69020.

22. Poulsen SS, Knudsen KB, Jackson P, et al. Multi-walled carbon nanotube-physicochemical properties predict the systemic acute phase response following pulmonary exposure in mice. *PLoS One*. 2017;12(4):e0174167.

23. Poulsen SS, Saber AT, Williams A, et al. MWCNTs of different physicochemical properties cause similar inflammatory responses, but differences in transcriptional and histological markers of fibrosis in mouse lungs. *Toxicol Appl Pharmacol*. 2015;284(1):16-32.

24. Husain M, Wu D, Saber AT, et al. Intratracheally instilled titanium dioxide nanoparticles translocate to heart and liver and activate complement cascade in the heart of C57BL/6 mice. *Nanotoxicology*. 2015;9(8):1013-1022.

25. Dong Z, Wu T, Qin W, et al. Serum amyloid A directly accelerates the progression of atherosclerosis in apolipoprotein E-deficient mice. *Mol Med*. 2011;17(11–12):1357-1364.

26. Thompson JC, Jayne C, Thompson J, et al. A brief elevation of serum amyloid A is sufficient to increase atherosclerosis. *J Lipid Res*. 2015;56(2):286-293.

27. Thompson JC, Wilson PG, Shridas P, et al. Serum amyloid A3 is pro-atherogenic. *Atherosclerosis*. 2018;268:32-35.

28. Lee HY, Kim SD, Baek SH, et al. Serum amyloid A stimulates macrophage foam cell formation via lectin-like oxidized low-density lipoprotein receptor 1 upregulation. *Biochem Biophys Res Comm*. 2013;433(1):18-23.

29. Anthony D, Seow HJ, Uddin M, et al. Serum amyloid A promotes lung neutrophilia by increasing IL-17A levels in the mucosa and gammadelta T cells. *Am J Respir Crit Care Med*. 2013;188(2):179-186.

30. Ather JL, Ckless K, Martin R, et al. Serum amyloid A (SAA) activates the NLRP3 inflammasome and promotes T(H)17 allergic asthma in mice. *J Immunol*. 2011;187(1):64-73.

31. Cantin AM, Paquette B, Richter M, Larivee P. Albumin-mediated regulation of cellular glutathione and nuclear factor kappa B activation. *Am J Respir Crit Care Med*. 2000;162(4 Pt 1):1539-1546.

32. Jacobsen NR, Stoeger T, van den Brule S, et al. Acute and subacute pulmonary toxicity and mortality in mice after intratracheal instillation of ZnO nanoparticles in three laboratories. *Food Chem Toxicol*. 2015;85:84-95.

33. Jacobsen NR, Moller P, Jensen KA, et al. Lung inflammation and genotoxicity following pulmonary exposure to nanoparticles in ApoE-/- mice. *Part Fibre Toxicol*. 2009;6:2.

34. Husain M, Kyjovska ZO, Bourdon-Lacombe J, et al. Carbon black nanoparticles induce biphasic gene expression changes associated with inflammatory responses in the lungs of C57BL/6 mice following a single intratracheal instillation. *Toxicol Appl Pharmacol*. 2015;289(3):573-588.

35. Bengtson S, Knudsen KB, Kyjovska ZO, et al. Differences in inflammation and acute phase response but similar genotoxicity in mice following pulmonary exposure to graphene oxide and reduced graphene oxide. *PLoS One*. 2017;12(6):e0178355.

36. Christophersen DV, Jacobsen NR, Andersen MH, et al. Cardiovascular health effects of oral and pulmonary exposure to multi-walled carbon nanotubes in ApoE-deficient mice. *Toxicology*. 2016;371:29-40.

37. Lykkesfeldt J. Determination of malondialdehyde as dithiobarbituric acid adduct in biological samples by HPLC with fluorescence detection: comparison with ultraviolet-visible spectrophotometry. *Clin Chem*. 2001;47(9):1725-1727.

38. Kyjovska ZO, Jacobsen NR, Saber AT, et al. DNA strand breaks, acute phase response and inflammation following pulmonary exposure by instillation to the diesel exhaust particle NIST1650b in mice. *Mutagenesis*. 2015;30(4):499-507.

39. Livak KJ, Schmittgen TD. Analysis of relative gene expression data using real-time quantitative PCR and the 2(-Delta Delta C(T)) Method. *Methods*. 2001;25(4):402-408.

40. Cao Y, Jacobsen NR, Danielsen PH, et al. Vascular effects of multiwalled carbon nanotubes in dyslipidemic ApoE-/- mice and cultured endothelial cells. *Toxicol Sci*. 2014;138(1):104-116.

41. Miller MR. The role of oxidative stress in the cardiovascular actions of particulate air pollution. *Biochem Soc Trans*. 2014;42(4):1006-1011.

42. Badolato R, Wang JM, Murphy WJ, et al. Serum amyloid A is a chemoattractant: induction of migration, adhesion, and tissue infiltration of monocytes and polymorphonuclear leukocytes. *J Exp Med*. 1994;180(1):203-209.

43. Lindhorst E, Young D, Bagshaw W, Hyland M, Kisilevsky R. Acute inflammation, acute phase serum amyloid A and cholesterol metabolism in the mouse. *Biochem Biophys Acta*. 1997;1339(1):143-154.

44. Saber AT, Koponen IK, Jensen KA, et al. Inflammatory and genotoxic effects of sanding dust generated from nanoparticle-containing paints and lacquers. *Nanotoxicology*. 2012;6(7):776-788.

45. Poulsen SS, Jackson P, Kling K, et al. Multi-walled carbon nanotube physicochemical properties predict pulmonary inflammation and genotoxicity. *Nanotoxicology*. 2016;10(9):1263-1275.

46. Hadrup N, Knudsen KB, Berthing T, et al. Pulmonary effects of nanofibrillated celluloses in mice suggest that carboxylation lowers the inflammatory and acute phase responses. *Environ Toxicol Pharmacol*. 2019;66:116-125.

47. Danielsen PH, Knudsen KB, Štrancar J, et al. Effects of physicochemical properties of TiO2 nanomaterials for pulmonary inflammation, acute phase response and alveolar proteinosis in intratracheally exposed mice. *Toxicol Appl Pharmacol*. 2020;386:114830.

48. Hayek T, Oiknine J, Brook JG, Aviram M. Increased plasma and lipoprotein lipid peroxidation in apo E-deficient mice. *Biochem Biophys Res Comm*. 1994;201(3):1567-1574.

49. Palinski W, Rosenfeld ME, Yla-Herttuala S, et al. Low density lipoprotein undergoes oxidative modification in vivo. *Proc Natl Acad Sci U S A*. 1989;86(4):1372-1376.

50. Torzewski M, Klouche M, Hock J, et al. Immunohistochemical demonstration of enzymatically modified human LDL and its colocalization with the terminal complement complex in the early atherosclerotic lesion. *Arterioscler Thromb Vasc Biol*. 1998;18(3):369-378.

51. Rye KA, Bursill CA, Lambert G, Tabet F, Barter PJ. The metabolism and anti-atherogenic properties of HDL. *J Lipid Res*. 2009;50(Suppl):S195-200.

52. Li R, Navab M, Pakbin P, et al. Ambient ultrafine particles alter lipid metabolism and HDL anti-oxidant capacity in LDLR-null mice. *J Lipid Res*. 2013;54(6):1608-1615.

53. Morgantini C, Natali A, Boldrini B, et al. Anti-inflammatory and antioxidant properties of HDLs are impaired in Type 2 diabetes. *Diabetes*. 2011;60(10):2617-2623.

54. Navab M, Anantharamaiah GM, Hama S, et al. Oral administration of an Apo A-I mimetic Peptide synthesized from D-amino acids dramatically reduces atherosclerosis in mice independent of plasma cholesterol. *Circulation*. 2002;105(3):290-292.

55. De Beer MC, Wroblewski JM, Noffsinger VP, et al. Deficiency of endogenous acute phase serum amyloid A does not affect atherosclerotic lesions in apolipoprotein E-deficient mice. *Arterioscler Thromb Vasc Biol*. 2014;34(2):255-261.